

## SEASONAL AND SECULAR VARIATIONS OF ATMOSPHERIC $^{14}\text{CO}_2$ OVER THE WESTERN PACIFIC SINCE 1994

H Kitagawa<sup>1</sup> • Hitoshi Mukai<sup>2</sup> • Yukihiro Nojiri<sup>2</sup> • Yasuyuki Shibata<sup>2</sup> • Toshiyuki Kobayashi<sup>2</sup> • Tomoko Nojiri<sup>3</sup>

**ABSTRACT.** Air sample collections over the western Pacific have continued since 1992 as a part of Center for Global Environmental Research, National Institute for Environmental Studies (CGER-NIES) global environmental monitoring program. The air samples collected on the Japan-Australia transect made it possible to trace the seasonal and secular  $^{14}\text{CO}_2$  variations, as well as an increasing trend of greenhouse gases over the western Pacific. A subset of  $\text{CO}_2$  samples from latitudes of 10–15°N and 23–28°S were chosen for accelerator mass spectrometry (AMS)  $^{14}\text{C}$  analysis using a NIES-TERRA AMS with a 0.3–0.4% precision. These  $^{14}\text{CO}_2$  records in maritime air show seasonal variations superimposed on normal exponential decreasing trends with a time constant of about 16 yr. The  $\Delta^{14}\text{C}$  values in the Northern Hemisphere are lower than those in the Southern Hemisphere by 3–4‰ during 1994–2002. The Northern Hemisphere record shows relatively high seasonality ( $2.3 \pm 1.5\%$ ) as compared with the Southern Hemisphere ( $1.3 \pm 1.2\%$ ). The maximum values of seasonal cycles appear in late autumn and early winter in the Northern and Southern Hemispheres, respectively. Oscillations of 1–10 yr over the western Pacific are found to correlate possibly with the El Niño/Southern Oscillation (ENSO) events.

### INTRODUCTION

The tropospheric radiocarbon concentration (represented by  $\Delta^{14}\text{C}$ , which includes a normalization for mass dependent fractionation and decay) has been monitored at islands and continental stations (Nydal and Lovseth 1983; Levin et al. 1980; Vogel 1970; Manning et al. 1990; Meijer et al. 1995; Levin et al. 1989, 1995). It almost doubled from its natural value during the early 1960s due to injection of  $^{14}\text{C}$  from thermonuclear bomb testing. At that time, troposphere-stratosphere exchange was a dominant contributor to produce seasonal and latitudinal variations in troposphere  $\Delta^{14}\text{C}$ . After the global moratorium on atmospheric nuclear testing following the Test Ban Treaty in 1963,  $\Delta^{14}\text{C}$  has decreased mainly through air-sea exchanges of  $\text{CO}_2$ , transfer to the biosphere, and dilution with fossil-fuel  $^{14}\text{C}$ -free  $\text{CO}_2$ , with an approximate exponential trend. The bomb  $^{14}\text{C}$  anomaly in the atmosphere has been used as a transient tracer for studying the global carbon cycle. By the late 1990s, the tropospheric  $\Delta^{14}\text{C}$  value reflects the distribution of natural and anthropogenic  $\text{CO}_2$  source and sinks (Rozanski et al. 1995; Meijer et al. 1995; Levin and Hesshaimer 2000). This information has provided independent information on the global  $\text{CO}_2$  source and sinks through the carbon-cycle modeling exercise (e.g. Randerson et al. 2002).

The air collections in the Japan and Australia transect have been made since 1992 as a part of the ongoing studies on a greenhouse gases monitoring program. The  $\Delta^{14}\text{C}$  changes in maritime air over the western Pacific from latitudes of 10–15°N and 23–28°S were determined for 1994–2002. Here, we made a comparison of those  $\Delta^{14}\text{C}$  records that could be characterized as “natural background.”

### METHODS

$\text{CO}_2$  has been continuously collected by an automatic sampler installed on container freighters at the 24 sites on the Japan and Australia transect since 1992. It was started by the Hakuba-maru (NYK line) from 1992. The ship was changed to the Southern Cross-maru (MOL line) in 1996 and again changed to the Golden Wattle (MOL line) in 2001. Air samplings on the Japan and Australia transect

<sup>1</sup>Graduate School of Environmental Studies, Nagoya University, Nagoya 464-8601, Japan. Corresponding author. Email: kitagawa@ihis.nagoya-u.ac.jp.

<sup>2</sup>National Institute for Environmental Studies, Tsukuba, Ibaraki 305-8506, Japan.

<sup>3</sup>Global Environmental Forum, c/o National Institute for Environmental Studies, Tsukuba, Ibaraki 305-8506, Japan.

were performed at approximately 3° latitude with a frequency of 6–10 times per yr. Air samples were collected in stainless steel containers (3.3 L in volume) at approximately +2.5 atm were picked up when the cargo ships arrived in ports quickly.

In the laboratory, CO<sub>2</sub> was cryogenically separated from about 6 L of air in a vacuum line after the determination of the concentrations of greenhouse gases such as CO<sub>2</sub>, CH<sub>4</sub>, and N<sub>2</sub>O. More than 1000 samples are kept as pure CO<sub>2</sub> in sealed glass tubes for the ongoing measurements of δ<sup>13</sup>C and <sup>14</sup>C contents. A subset of CO<sub>2</sub> samples collected at the latitudes of 10–15°S and 23–28°N was converted to graphite for accelerator mass spectrometry (AMS) <sup>14</sup>C measurements. <sup>14</sup>C/<sup>12</sup>C and <sup>13</sup>C/<sup>12</sup>C ratios (for the isotope fractionation correction) were determined using the NIES-TERRA AMS. The <sup>14</sup>C contents are reported as the permil notation (Δ<sup>14</sup>C ‰) following standard convention (Stuiver and Polach 1977) after normalizing to isotope fractionation and correction for decay. Typical 1-σ precision on Δ<sup>14</sup>C is about ±5‰.

## RESULTS AND DISCUSSION

Δ<sup>14</sup>C data from the 2 areas are plotted with CO<sub>2</sub> concentration data (Figure 1). We give the Δ<sup>14</sup>C and CO<sub>2</sub> concentration data in the Appendix. The main feature of Δ<sup>14</sup>C records is the existence of seasonality superimposed on normal exponential decreasing trends with a decay (or e-folding) time constant (*t*). To isolate the secular and seasonal components in the Δ<sup>14</sup>C time series, the seasonal component is expressed by single harmonic function (*A cos [2π*t* / *T* + φ]*, where *A* and φ are constants), and all the data is fitted to the following formula:

$$\Delta^{14}C_t = \Delta^{14}C_{1994} e^{-\Delta t/\tau} + A \cos (2\pi t / T + \varphi) \quad (1),$$

where Δ<sup>14</sup>C<sub>*t*</sub> is the measured value in given time (*t*) and Δ*t* is the time since 1994 (the base year). The fitting parameters were obtained by the nonlinear least-squares method using a Levenberg-Marquardt algorithm. The fits are shown in Figure 1, while the fitted parameters are shown in Table 1.

### Trend of Δ<sup>14</sup>C Over the Western Pacific

Δ<sup>14</sup>C values in maritime air over the western Pacific show a gradual decreasing in both hemispheres, corresponding to the exponential decreasing of global Δ<sup>14</sup>C trend due to the Suess effect (Levin and Hesshaimer 2000). The average e-fold time constants during 1994–2002 in the Northern and Southern Hemisphere over the western Pacific are, respectively, 15.6 ± 1.3 yr (Δ<sup>14</sup>C is 128.4 ± 3.2‰ in January 1994) and 16.4 ± 0.9 yr (Δ<sup>14</sup>C is 133.7 ± 2.3‰ in January 1994). The reported e-fold time constant is about 16 yr for the Northern Hemisphere (Levin and Kromer 1997) and about 17 yr for the Southern Hemisphere (Manning et al. 1990). The decreasing trend of Δ<sup>14</sup>C over the western Pacific agrees well with that from other area during the 1990s.

### Absolute Values

To assess the N-S offset of Δ<sup>14</sup>C over the western Pacific, we compared 2 curves shown in Figure 1. As expected, the absolute Δ<sup>14</sup>C values in the Northern Hemisphere are lower than those in the Southern Hemisphere by 3.3‰ on average, and they do not show the apparently systematical shift with time for 1994–2002. Surface observation at the globally distributed background stations located between 82°N (Alert, Nunavut, Canada) and 7°S (Neumayer, Antarctica) suggests that the N-S Δ<sup>14</sup>C gradient is nearly zero in the early 1990s (Levin and Hesshaimer 2000). The model calculation predicts that the N-S offset will be expanded, with the Northern Hemisphere becoming progressively more <sup>14</sup>C-depleted as compared with the Southern Hemisphere in the coming year (Randerson et al. 2002). Our observation supports the model prediction that Δ<sup>14</sup>C in the Northern Hemisphere will decrease from the direct input of fossil-fuel emissions with an isotope signal of –1000‰.

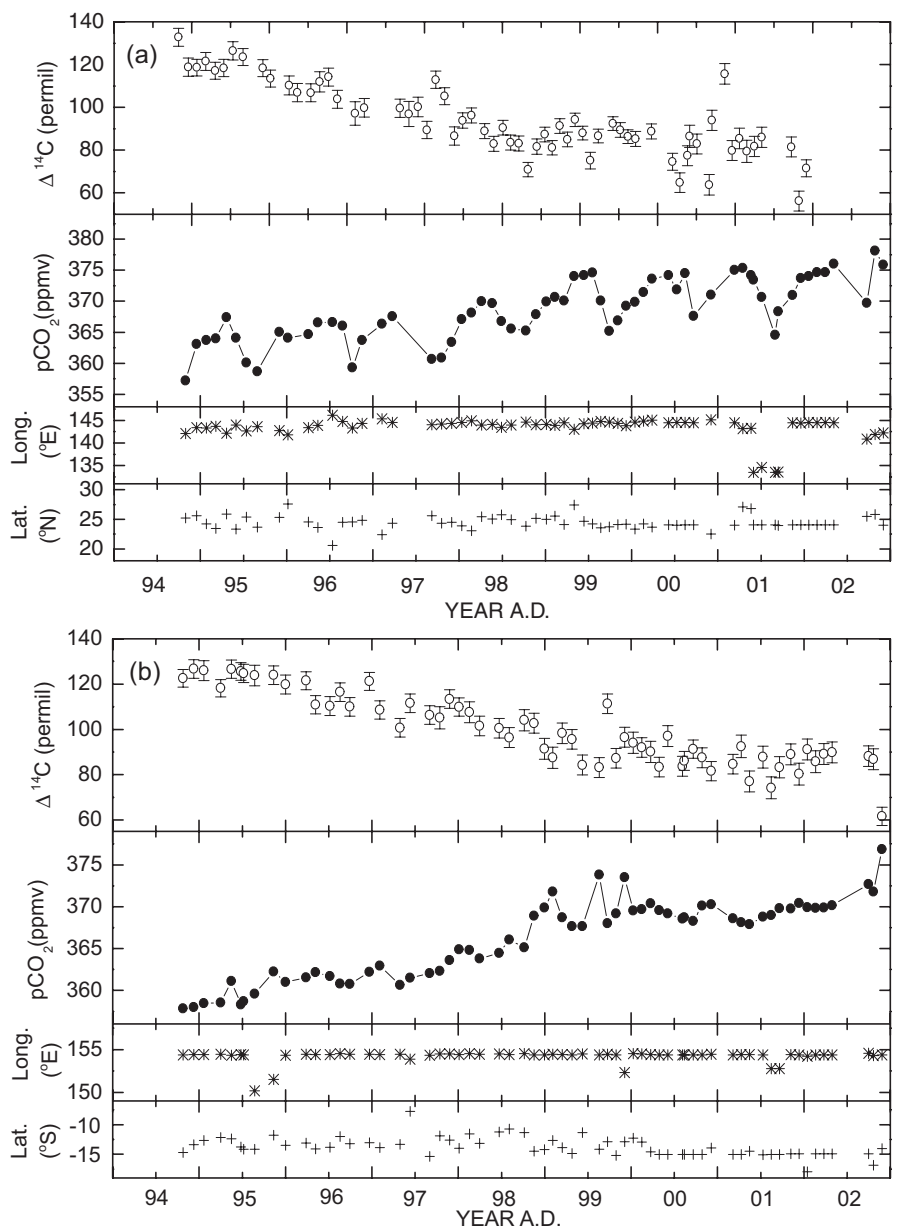


Figure 1  $\Delta^{14}\text{C}$  and  $\text{CO}_2$  concentration in maritime air collected at the latitudes of 23–28°N (above) and 10–15°S (below) over the western Pacific.

**Seasonality**

The decreasing trend of the seasonal cycle was assessed using Equation 1. The Northern Hemisphere record shows higher seasonality ( $2.3 \pm 1.5\%$ ) as compared with the Southern Hemisphere ( $1.3 \pm 1.2\%$ ). The larger seasonal variations were reported at observation stations in the Northern Hemisphere, where they are strongly influenced by the anthropologically induced  $\text{CO}_2$  emissions (Levin et al. 1989, 1995; Meijer et al. 1995). In remote stations, fossil-fuel emission is little, e.g.,

only <5‰ on peak-to-peak basis at Izana in Canary Island, which is consistent with our results. The  $\Delta^{14}\text{C}$  data discussed here could be regarded as “natural background.”

The amplitudes of the seasonal cycle are close to the  $\Delta^{14}\text{C}$  measurement error. It should be noted that the estimated phases of seasonal cycles have a margin of error (Table 1). The maximum  $\Delta^{14}\text{C}$  values appear roughly in October and December in the Northern and Southern Hemispheres, respectively, when the atmospheric  $\text{CO}_2$  concentration is lower in the Northern Hemisphere (Figure 1). There seems to be a small N-S difference in phase by about 2 months. Interestingly, the  $\Delta^{14}\text{C}$  records from the Northern Hemisphere (10–15°N) over the western Pacific are somewhat out of phase with those of Izana, Tenerife Island (28°N) in the Atlantic (with the maximum in middle July [Meyer et al. 1995]).

Table 1 Characteristics of the fitted seasonal and exponential decreasing changes. The  $\Delta^{14}\text{C}$  measurement series from the Northern and Southern Hemispheres were fitted to the formula,  $\Delta^{14}\text{C}_t = \Delta^{14}\text{C}_{1994} e^{-\Delta t/\tau} + A \cos(2\pi t / T + \varphi)$ .

Area	$\Delta^{14}\text{C}_{1994}$ (‰)	Decay time constant ( $\tau$ , year)	Amplitude (A, ‰)	Phase ( $\varphi$ , maximum)
23–28°N	128.4 ± 3.2	15.6 ± 1.3	2.3 ± 1.5	Oct 10 (±40 days)
10–15°S	133.7 ± 2.3	16.4 ± 0.9	1.3 ± 1.2	Dec 10 (±50 days)

The seasonality of tropospheric  $\Delta^{14}\text{C}$  is sensitive to fossil-fuel emissions, ocean-atmosphere exchanges, stratosphere-troposphere mixing, and terrestrial-ecosystem fluxes (Nydel and Lovseth 1983; Enting and Mansbridge 1987). Seasonal cycles in the 1960s were produced by stratosphere-troposphere exchange because stratospheric  $^{14}\text{C}$  fluxes are injected into the upper troposphere in April and May in the Northern Hemisphere (Appenzeller et al. 1996). Model analyses of the stratosphere-troposphere exchange could not explain our result for the phase of seasonal cycles (Manning et al. 1990). In later decades, the records from European continental stations show clear seasonal cycles, caused probably by the summer-winter difference in fossil-fuel emissions (Levin et al. 1989; Meijer et al. 1995). The seasonal cycle (with the maximum in middle October and middle December over the western Pacific) is out of phase with that of the European continental stations; the continental stations' maximum occurs during middle July and late August and coincides with the warmest period of summer in the Northern Hemisphere. The direct impact of fossil-fuel  $^{14}\text{C}$ -free  $\text{CO}_2$  would be a minor contributor to the seasonal cycle over the western Pacific. The phase reverse of  $\Delta^{14}\text{C}$  and  $\text{CO}_2$  concentration cycles in the Northern Hemisphere may be caused by net  $\text{CO}_2$  fluxes from terrestrial ecosystems and ocean exchanges, as suggested by model prediction (Randerson et al. 2002).

### 1–10 Year Oscillations

The residual of  $\Delta^{14}\text{C}$  ( $\Delta^{14}\text{C}_{res}$ ) was calculated as the difference between measured values and each fitted curve (Figure 2). The standard deviation of  $\Delta^{14}\text{C}_{res}$  values during 1994–2002 is 8.9‰ and 6.2‰ in the Northern and Southern Hemispheres, respectively.  $\Delta^{14}\text{C}_{res}$  records from 2 areas show a weak coincidence in the general trends. Although more data are needed to verify the presence of the 1–10 year oscillations of  $\Delta^{14}\text{C}_{res}$ , the existence of 1–10 year oscillations of  $\Delta^{14}\text{C}$  may be a common feature, at least over the tropical western Pacific.

The 1–10 year oscillations of tropospheric  $\Delta^{14}\text{C}$  during the post- and pre-nuclear era are reported. Spectrum analysis of the annual high-precision  $^{14}\text{C}$  time series from tree rings of Washington and Arizona (AD 1511–1954) show periodicities in the 2–6.4 yr ranges, potentially associating with ENSO-related thermohaline circulation changes (Stuiver and Braziunas 1993). In the post-nuclear

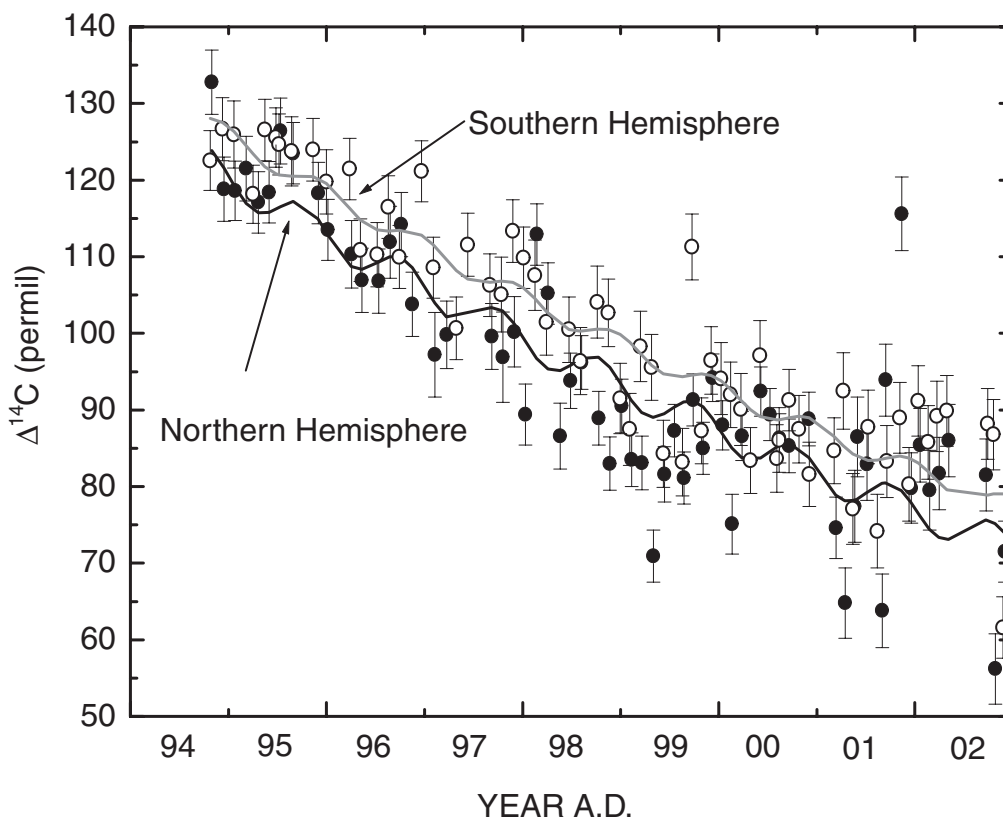


Figure 2 Comparison of  $\Delta^{14}\text{C}$  records from the Northern and Southern Hemispheric air, fitted with a combined normal exponential and single harmonic curve for the years 1994–2002. Filled and open circles with a  $\pm 1\text{-}\sigma$  error bar are from the Northern and Southern Hemispheres, respectively.

era,  $\Delta^{14}\text{C}$  changes on a regional scale by ENSO events are also observed in the equatorial Pacific region between 1991–1993 (Rozanski et al. 1995).

In Figure 3, the  $\Delta^{14}\text{C}_{res}$  over the western Pacific are compared with the Tahiti-Darwin Southern Oscillation (SOI) (Ropelewski and Jones 1987) and the Multi-Variate ENSO index (MEI) (Wolter and Timlin 1998). The overall  $\Delta^{14}\text{C}_{res}$  trend (relatively high around 1997–1998 and increasing after late 1998) is potentially correlated with the ENSO events.

El Niño events are characterized by anomalously warm sea surface temperature in the equatorial Pacific. The events can cause significant perturbation in the global carbon cycles, such as changes in the ocean-atmosphere  $\text{CO}_2$  exchange and terrestrial  $\text{CO}_2$  fluxes (Keeling et al. 1995). The weakened thermocline circulation in the equatorial Pacific during El Niño events can generate significant reduction in the upwelling of  $\text{CO}_2$ -rich deep-water mass and in the sea-air efflux of  $\text{CO}_2$  by 30–80% from the normal condition (Feely et al. 1999). In addition, El Niño events are also accompanied by anomalous atmospheric circulation patterns, resulting potentially in enhanced biospheric  $\text{CO}_2$  flux due to reduction in rainfall in tropical rainforests (Prentice and Lloyd 1998) and in enhanced transport of stratospheric air with higher  $\Delta^{14}\text{C}$  (Nakamura et al. 1992) to the troposphere. All these phenomena may be related to the positive anomaly of the  $\Delta^{14}\text{C}_{res}$  record over the western Pacific during 1997–1998. After the ENSO event, the arid condition in tropical rainforests poten-

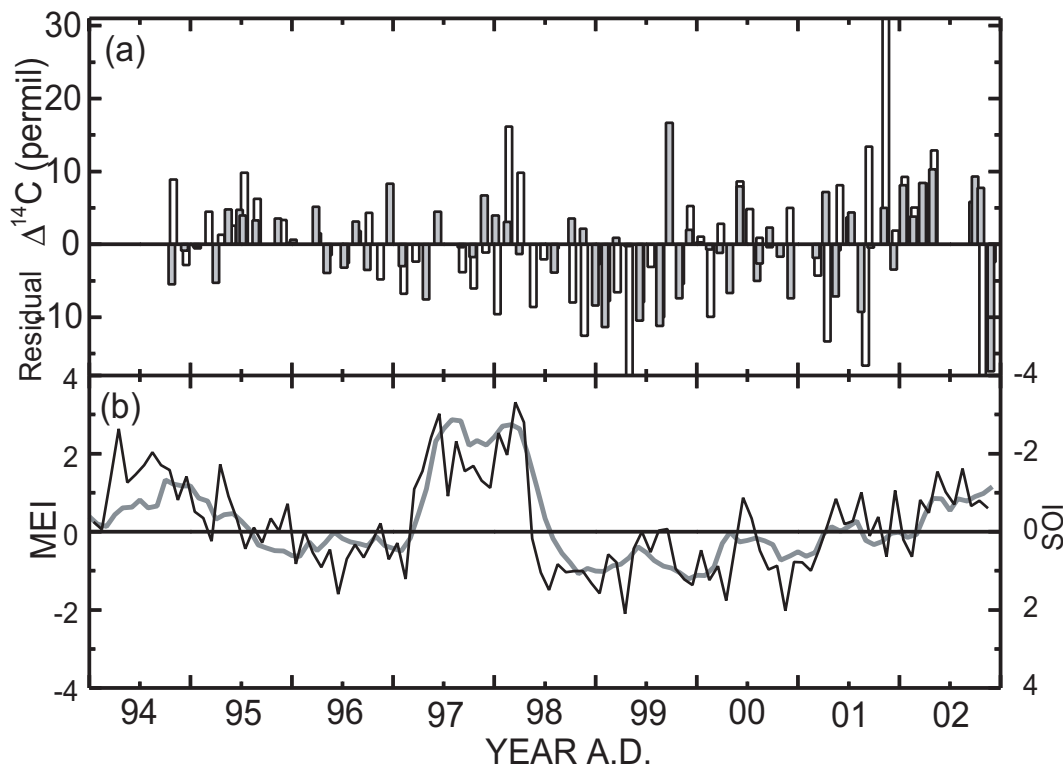


Figure 3 (a) Residual  $\Delta^{14}\text{C}$  record calculated as the differences between the measured values and fitted curves. The residual  $\Delta^{14}\text{C}$  values from the Northern and Southern Hemisphere are shown by open and gray bars, respectively; (b) The thick black and thin gray lines are monthly multi-variate ENSO index (MEI) (Wolter and Timlin 1998) and Tahiti-Darwin Southern Oscillation (SOI) (Ropelewski and Jones 1987), respectively. Positive MEI and negative SOI values represent the El Niño condition.

tially can release  $^{14}\text{C}$ -rich  $\text{CO}_2$  from the fast cycling soil organic matters with a time lag (Payner et al. 1998). The gradual increasing in  $\Delta^{14}\text{C}_{\text{res}}$  after the 1997–1998 ENSO event seems to be related to such a biospheric release of  $^{14}\text{C}$ -enriched  $\text{CO}_2$ .

## CONCLUSION

Our observations revealed the 3 timescale changes of  $\Delta^{14}\text{C}$  of atmospheric  $\text{CO}_2$  that could be characterized as “natural background.” The ongoing measurements of the samples from the different latitudes on the Japan–Australia transect over the western Pacific will give new insights to quantitatively understand the role of the terrestrial biosphere and ocean as a sink of anthropogenic  $\text{CO}_2$  emissions in the past and in the coming years.

## REFERENCES

- Appenzeller C, Holton JR, Rosenlof KH. 1996. Seasonal variation of mass transport process across the tropopause. *Journal of Geophysical Research* 101(D10): 15,071–8.
- Feeley RA, Wanninkhof R, Takahashi T, Tans P. 1999. The influence of El Niño on the equatorial Pacific contribution to atmospheric  $\text{CO}_2$  accumulation. *Nature* 398: 597–601.
- Keeling CD, Whorf TP, Wahlen M, van der Plicht J. 1995. Interannual extremes in the rate of rise of atmospheric carbon dioxide since 1980. *Nature* 398:666–70.
- Levin I, Graul R, Trivett NBA. 1995. Long-term observations of atmospheric  $\text{CO}_2$  and carbon isotopes at continental sites in Germany. *Tellus* 47B(1/2):23–4.

- Levin I, Heshaimer V. 2000. Radiocarbon—a unique tracer of global carbon cycle dynamics. *Radiocarbon* 42(1):69–80.
- Levin I, Kromer B. 1997. Twenty years of atmospheric  $^{14}\text{CO}_2$  observations at Schauinsland station, Germany. *Radiocarbon* 39(2):205–18.
- Levin I, Münnich KO, Weiss W. 1980. The effect of anthropogenic  $\text{CO}_2$  and  $^{14}\text{C}$  sources on the distribution of  $^{14}\text{C}$  in the atmosphere. In: Stuiver M, Kra RS, editors. Proceedings of the 10th International  $^{14}\text{C}$  Conference. *Radiocarbon* 22(2):379–91.
- Levin I, Schuchard J, Kromer B, Münnich KO. 1989. The continental European Suess effect. *Radiocarbon* 31(3):431–40.
- Manning MR, Lowe DC, Melhuish WH, Sparks RJ, Wallace G, Brenninkmeijer CAM, McGill RC. 1990. The use of radiocarbon measurements in atmospheric studies. *Radiocarbon* 32(1):37–58.
- Meijer HA, van der Plicht J, Gislefoss JS, Nydal R. 1995. Comparing long-term atmospheric  $^{14}\text{C}$  and  $^3\text{H}$  records near Groningen, the Netherlands with Fruholmen, Norway and Izana, Canary Islands  $^{14}\text{C}$  station. *Radiocarbon* 37(1):39–50.
- Nakamura T, Nakazawa T, Nakai N, Kitagawa H, Honda H, Itoh T, Machida T, Matsumoto E. 1992. Measurement of  $^{14}\text{C}$  concentrations of stratospheric  $\text{CO}_2$  by accelerator mass spectrometry. *Radiocarbon* 34(3):745–52.
- Nydal R, Lovseth K. 1983. Tracing bomb  $^{14}\text{C}$  in the atmosphere 1962–1980. *Journal of Geophysical Research* 88:3621–42.
- Payner PJ, Law RM, Dragaville R. 1998. The relationship between tropical  $\text{CO}_2$  fluxes and the El Niño–Southern Oscillation. *Geophysical Research Letters* 26:493–6.
- Prentice IC, Lloyd JC. 1998. C-Quest in the Amazon Basin. *Nature* 396:619–20.
- Randerson JT, Enting IG, Schuur EAG, Caldeira K, Fung IY. 2002. Seasonal and latitudinal variability of troposphere  $\Delta^{14}\text{CO}_2$ : post-bomb contributions from fossil fuels, oceans, the stratosphere, and the terrestrial biosphere. *Global Biogeochemical Cycles* 16:1112–31.
- Ropelewski CF, Jones PD. 1987. An extension of the Tahiti–Darwin Southern Oscillation Index. *Monthly Weather Review* 115:2161–5. <http://www.cru.uea.ac.uk/cru/data/soi.htm>.
- Rozanski K, Levin I, Stock J, Falcon REG, Rubio F. 1995. Atmospheric  $^{14}\text{CO}_2$  variations in the equatorial region. *Radiocarbon* 37(2):509–15.
- Stuiver M, Braziunas TF. 1993. Sun, ocean, climate and atmospheric  $^{14}\text{CO}_2$ : an evolution of causal and spectral relationships. *The Holocene* 3:289–305.
- Stuiver M, Polach HA. 1997. Discussion: reporting of  $^{14}\text{C}$  data. *Radiocarbon* 19(3):355–63.
- Vogel JC. 1970. Groningen radiocarbon dates IX. *Radiocarbon* 12(2):444–71.
- Wolter K, Timlin MS. 1998. Measuring the strength of ENSO—how does 1997/98 rank? *Weather* 53:315–24. <http://www.cdc.noaa.gov/cru/~kew/MEI/mei.htm>.



Appendix <sup>14</sup>C data list.

ID	Date	Lat (°N)	Long (°E)	pCO <sub>2</sub> (ppmv)	Δ <sup>14</sup> C (‰)	Δ <sup>14</sup> C <sub>unc</sub> (‰)	
H06-05	C2	30-Oct-94	25.20	142.12	357.20	132.8	4.2
H06-06	C4	15-Dec-94	25.58	143.40	363.10	118.8	4.2
H06-07	C2	25-Jan-95	24.20	143.30	363.70	118.6	3.9
H06-08	C3	7-Mar-95	23.47	143.67	364.00	121.5	4.2
H07-01	C3	21-Apr-95	25.90	142.17	367.40	117.1	4.0
H07-02	C2	31-May-95	23.37	143.95	364.10	118.4	4.0
H07-03	C4	13-Jul-95	25.40	142.68	360.10	126.4	4.3
H07-04	C1	29-Aug-95	23.68	143.60	358.70	123.5	4.0
H07-06	C3	24-Nov-95	25.30	142.77	365.05	118.3	4.0
H07-07	C6	6-Jan-96	27.57	141.80	364.11	113.5	4.0
H08-01	C5	2-Apr-96	24.58	143.37	364.68	110.3	4.4
H08-02	C4	12-May-96	23.64	143.87	366.56	106.9	4.2
H08-03	C3	13-Jul-96	20.60	146.11	366.62	106.8	4.2
H08-04	C5	24-Aug-96	24.48	144.79	366.05	111.9	4.7
H08-05	C6	5-Oct-96	24.58	143.35	359.30	114.2	4.2
H08-06	C4	16-Nov-96	24.85	144.33	363.73	103.8	4.2
H08-08	C4	8-Feb-97	22.42	145.37	366.35	97.2	5.5
H08-09	C4	23-Mar-97	24.33	144.56	367.57	99.8	4.4
H09-04	C4	7-Sep-97	25.58	144.05	360.69	99.6	4.3
H09-05	C3	18-Oct-97	24.33	144.21	360.89	96.9	5.9
H09-06	C4	30-Nov-97	24.50	144.33	363.42	100.2	4.6
H09-07	C5	11-Jan-98	23.92	144.57	367.07	89.4	4.0
H09-08	C5	22-Feb-98	23.07	144.92	368.12	112.9	4.0
H10-01	C5	5-Apr-98	25.43	143.95	369.96	105.2	4.0
H10-02	C3	20-May-98	25.06	144.08	369.66	86.6	4.3
H10-03	C5	28-Jun-98	25.77	143.46	366.77	93.8	3.6
H10-04	C3	8-Aug-98	24.92	143.96	365.55	96.2	3.5
H10-05	C3	10-Oct-98	23.85	144.58	365.24	88.9	3.5
H10-06	C3	21-Nov-98	25.14	144.03	367.88	83.0	3.5
H10-07	C3	4-Jan-99	24.97	144.13	369.90	90.5	3.5
H10-08	C4	9-Feb-99	25.53	143.87	370.68	83.5	3.5
H10-09	C4	20-Mar-99	24.10	144.50	370.10	83.1	3.5
H11-01	C4	2-May-99	27.43	143.06	374.03	70.9	3.4
H11-02	C3	12-Jun-99	24.69	144.24	374.19	81.6	3.6
H11-03	C3	19-Jul-99	24.22	144.43	374.62	87.3	3.4
H11-04	C2	23-Aug-99	23.57	144.73	370.08	81.1	3.4
H11-05	C3	27-Sep-99	23.71	144.65	365.17	91.3	3.4
H11-06	C4	3-Nov-99	24.09	144.36	366.87	85.0	3.4
H11-07	C4	8-Dec-99	24.17	143.80	369.23	94.2	3.1
H11-08	C4	14-Jan-00	23.32	144.65	369.84	88.0	3.2
H11-09	C4	19-Feb-00	24.21	144.83	371.45	75.1	3.9
H11-10	C3	28-Mar-00	23.66	145.07	373.62	86.6	3.2
H12-02	C4	5-Jun-00	24.04	144.50	374.15	92.4	3.2
H12-03	C4	10-Jul-00	24.03	144.51	371.87	89.4	3.4
H12-04	C4	14-Aug-00	24.04	144.51	374.47	86.3	3.2
H12-05	C4	19-Sep-00	24.04	144.49	367.62	85.3	3.5



Appendix  $^{14}\text{C}$  data list. (Continued)

ID	Date	Lat (°N)	Long (°E)	pCO <sub>2</sub> (ppmv)	$\Delta^{14}\text{C}$ (‰)	$\Delta^{14}\text{C}_{\text{unc}}$ (‰)	
H12-07	C6	2-Dec-00	22.53	145.15	371.03	88.8	3.5
H12-10	C4	12-Mar-01	24.03	144.49	375.01	74.6	4.0
H13-01	C5	16-Apr-01	27.07	143.19	375.31	64.8	4.6
H13-02	C5	21-May-01	26.83	143.28	374.18	77.4	4.7
H13-03	A4	31-May-01	24.04	133.55	373.44	86.5	5.2
H13-04	A4	5-Jul-01	24.05	134.63	370.65	82.9	4.7
H13-05	A4	9-Aug-01	24.04	133.51	364.58	63.8	4.8
H13-06	A4	13-Sep-01	23.95	133.57	368.36	93.9	4.7
H13-07	C4	12-Nov-01	24.05	144.50	370.96	115.6	4.8
H13-08	C4	17-Dec-01	24.06	144.43	373.69	79.8	4.6
H13-09	C4	20-Jan-02	24.05	144.57	374.03	85.4	4.8
H13-10	C4	24-Feb-02	24.06	144.48	374.66	79.5	5.2
H14-01	C4	31-Mar-02	24.05	144.51	374.63	81.7	4.7
H14-02	C4	6-May-02	24.05	144.49	376.03	86.0	4.7
H14-03	C4	22-Sep-02	25.50	140.90	369.72	81.5	4.7
H14-04	C4	27-Oct-02	25.80	141.85	378.10	56.2	4.6
H14-05	C4	1-Dec-02	24.03	142.22	375.85	71.5	4.0
H06-05	A2	24-Oct-94	-14.72	154.37	357.85	122.6	3.9
H06-06	A5	9-Dec-94	-13.38	154.42	357.98	126.7	4.1
H06-07	A4	20-Jan-95	-12.65	154.43	358.47	126	4.4
H06-08	A5	1-Mar-95	-12.18	154.47	358.53	118.2	3.8
H07-01	A4	16-Apr-95	-12.37	154.35	361.10	126.6	4
H07-02	A4	26-May-95	-13.75	154.42	358.31	125.6	3.9
H07-03	A4	7-Jul-95	-14.15	154.37	358.70	124.7	4
H07-04	A2	23-Aug-95	-14.17	150.17	359.58	123.8	4.5
H07-06	A4	19-Nov-95	-11.80	151.52	362.23	124	4.1
H07-07	A6	31-Dec-95	-13.50	154.32	360.98	119.8	4.2
H08-01	A6	27-Mar-96	-13.08	154.47	361.55	121.5	4
H08-02	A5	6-May-96	-14.10	154.41	362.16	110.9	4.1
H08-03	A5	7-Jul-96	-13.80	154.41	361.68	110.3	4.2
H08-04	A6	18-Aug-96	-12.01	154.52	360.81	116.5	4.1
H08-05	A6	29-Sep-96	-13.19	154.46	360.75	110	4.1
H08-07	A5	20-Dec-96	-13.07	154.45	362.20	121.2	4
H08-08	A5	2-Feb-97	-13.88	154.41	362.93	108.6	4
H09-01	A5	28-Apr-97	-13.31	154.44	360.64	100.7	4.1
H09-02	A7	9-Jun-97	-7.76	153.89	361.49	111.6	4.1
H09-04	A5	31-Aug-97	-15.36	154.34	362.05	106.3	4.1
H09-05	A5	13-Oct-97	-11.88	154.50	362.33	105.1	4.9
H09-06	A5	24-Nov-97	-12.59	154.48	363.62	113.4	4.1
H09-07	A6	4-Jan-98	-13.96	154.42	364.87	109.9	4
H09-08	A5	16-Feb-98	-11.57	154.53	364.82	107.6	4.6
H10-01	A5	30-Mar-98	-13.17	154.44	363.78	101.5	4.3
H10-03	A5	22-Jun-98	-11.25	154.50	364.47	100.5	4.3
H10-04	A4	3-Aug-98	-10.71	154.40	366.07	96.4	4.4
H10-05	A4	5-Oct-98	-11.37	154.52	365.12	104.1	4.7
H10-06	A4	15-Nov-98	-14.49	154.37	368.89	102.7	4.4
H10-07	A5	29-Dec-98	-14.21	154.39	369.87	91.5	4.6
H10-08	A5	3-Feb-99	-12.66	154.47	371.79	87.5	4.7

Appendix <sup>14</sup>C data list. (Continued)

ID	Date	Lat (°N)	Long (°E)	pCO <sub>2</sub> (ppmv)	Δ <sup>14</sup> C (‰)	Δ <sup>14</sup> C <sub>unc</sub> (‰)	
H10-09	A5	14-Mar-99	-13.85	154.43	368.71	98.3	4.6
H11-01	A4	25-Apr-99	-14.85	154.36	367.64	95.6	4.3
H11-02	A4	7-Jun-99	-11.32	154.51	367.67	84.3	4.4
H11-04	A4	18-Aug-99	-14.17	154.38	373.82	83.2	4.4
H11-05	A5	22-Sep-99	-12.88	154.45	368.01	111.3	4.3
H11-06	A6	28-Oct-99	-15.21	154.39	369.16	87.3	4.3
H11-07	A5	3-Dec-99	-12.88	152.33	373.50	96.5	4.4
H11-08	A6	9-Jan-00	-12.30	154.54	369.52	94.1	4.7
H11-09	A5	13-Feb-00	-12.92	154.51	369.67	92	4.3
H11-10	A4	22-Mar-00	-14.61	154.42	370.38	90.1	4.7
H12-01	A5	26-Apr-00	-15.06	154.39	369.57	83.4	4.3
H12-02	A5	31-May-00	-15.06	154.39	369.16	97.1	4.6
H12-03	A5	5-Jul-00	-15.06	154.39	368.57	83.7	4.4
H12-04	A5	8-Aug-00	-15.06	154.39	368.71	86.1	4.2
H12-05	A5	13-Sep-00	-15.06	154.39	368.28	91.3	4.0
H12-06	A5	20-Oct-00	-15.06	154.38	370.10	87.5	4.4
H12-07	A7	26-Nov-00	-13.92	154.45	370.28	81.6	4.2
H12-10	A5	6-Mar-01	-15.06	154.39	368.58	84.7	4.3
H13-01	A5	10-Apr-01	-15.03	154.40	368.11	92.5	5.0
H13-02	A5	15-May-01	-14.50	154.43	367.89	77.1	4.6
H13-04	C3	11-Jul-01	-15.07	154.39	368.77	87.8	4.8
H13-05	C3	15-Aug-01	-15.06	152.79	368.97	74.2	4.8
H13-06	C3	19-Sep-01	-15.06	152.77	369.79	83.3	4.7
H13-07	A5	6-Nov-01	-14.94	154.40	369.75	89	4.6
H13-08	A5	11-Dec-01	-14.94	154.39	370.42	80.3	4.8
H13-09	A4	14-Jan-02	-17.93	154.23	369.91	91.2	4.6
H13-10	A5	19-Feb-02	-14.94	154.38	369.84	85.8	4.8
H14-01	A5	25-Mar-02	-14.94	154.39	369.89	89.2	4.6
H14-02	A5	30-Apr-02	-14.94	154.38	370.17	89.9	4.6
H14-03	A3	16-Sep-02	-14.92	154.57	372.68	88.2	4.6
H14-04	A3	21-Oct-02	-16.85	154.30	371.79	86.8	4.6
H14-05	A4	26-Nov-02	-14.03	154.38	376.85	61.6	4.0
H06-05	C2	30-Oct-94	25.20	142.12	357.20	132.8	4.2
H06-06	C4	15-Dec-94	25.58	143.40	363.10	118.8	4.2
H06-07	C2	25-Jan-95	24.20	143.30	363.70	118.6	3.9
H06-08	C3	7-Mar-95	23.47	143.67	364.00	121.5	4.2
H07-01	C3	21-Apr-95	25.90	142.17	367.40	117.1	4.0
H07-02	C2	31-May-95	23.37	143.95	364.10	118.4	4.0
H07-03	C4	13-Jul-95	25.40	142.68	360.10	126.4	4.3
H07-04	C1	29-Aug-95	23.68	143.60	358.70	123.5	4.0
H07-06	C3	24-Nov-95	25.30	142.77	365.05	118.3	4.0
H07-07	C6	6-Jan-96	27.57	141.80	364.11	113.5	4.0